Deposition, Clearance, and Translocation of Chrysotile Asbestos from Peripheral and Central Regions of the Rat Lung

PATRICK G. COIN,*,† VICTOR L. ROGGLI,† AND ARNOLD R. BRODY*

Laboratory of Pulmonary Pathobiology, National Institute of Environmental Health Sciences, Research Triangle Park, North Carolina 27709; and †Department of Pathology, Duke University and Durham Veterans Administration Medical Centers, Durham, North Carolina 27710

Received September 3, 1991

We investigated the pulmonary deposition, clearance, and translocation of chrysotile asbestos in the context of our previously developed model of asbestosis in the rat. Adult male rats were exposed for 3 hr to an aerosol of chrysotile asbestos. Subgroups were sacrificed up to 29 days postexposure and the lungs of the animals fixed. Peripheral and central regions of the left lung were resected, digested, and analyzed for fiber content by scanning electron microscopy. Pulmonary deposition did not differ between peripheral and central regions. There was no evidence of translocation of fibers from central to peripheral regions. The average diameter of retained fibers decreased over time, consistent with longitudinal splitting. The average length of retained fibers increased over time, consistent with slower clearance of longer fibers. We employed a novel counting scheme to ensure accurate fiber number measurements, allowing the calculation of clearance rates for fibers 0.5 to ≥16 μm in length. Fibers of length ≥16 μm were cleared slowly, if at all. These findings could have important implications for the pathogenesis of asbestos-related pleural disease. Many fibers are deposited in the peripheral region, and the longest (≥16 μm) will persist there for extended periods.

INTRODUCTION

Asbestos exposure causes disease in three regions of the respiratory system: carcinoma in the bronchial tree, asbestosis (i.e., fibrotic scarring) in the small airways and parenchyma, and both mesothelioma and fibrosis in the pleural region. Upon inhalation, fibers are deposited in both the bronchial tree and the parenchyma. In order to cause disease in the pleural region, fibers must presumably be translocated there after deposition. The mechanism and kinetics of this process are unknown (Hillerdal, 1980).

Previous work suggested that few fibers would be deposited in parenchymal regions adjacent to the visceral pleura. There is enhanced deposition of asbestos fibers at first alveolar duct bifurcations (Brody *et al.*, 1981), but these anatomic sites do not occur immediately adjacent to the visceral pleura. Deposition of fibers decreases with increasing airway pathlength and bifurcation number in the tracheobronchial and pulmonary regions of the rat lung (Pinkerton *et al.*, 1986). Warheit and Hartsky (1990) observed that deposition of carbonyl iron particles at alveolar duct bifurcations decreased distally from the terminal bronchioles toward the pleura, and the same pattern appears to hold for asbestos fibers (Brody and Roe, 1983).

Experimental work suggests that, in order to cause pleural disease, fibers must be present in the pleura or immediately adjacent regions of the pulmonary paren-

0013-9351/92 $5.00

chyma. For example, direct injection of fibers into the pleural or perito ities causes a high incidence of mesothelioma (Stanton *et al.*, 1981; Jaur 1987), suggesting that the mesothelium itself is the target tissue in tha Malignancy may also arise in mesenchymal cells underlying the visce (Hill *et al.*, 1990). In addition, some fibrotic pleural disease may be a con of inflammation in this subserosal layer (Dodson and Ford, 1985; Lap 1991).

Even though postdepositional movement (translocation) of fibers is i in the genesis of pleural disease, there have been few investigations translocation to the pleural region. Some studies in humans suggest tha fibers are translocated to the subpleural pulmonary parenchyma as we visceral and parietal pleura (Churg and Wiggs, 1987; Sebastien *et al.*, 198(and Kohyama, 1991). Viallat *et al.* (1986) recovered short (0.3–1.3 μ length) chrysotile fibers from the pleural cavity of rats in two peaks 7 to after an intratracheal instillation. Morgan *et al.* (1977) exposed rats for 3 aerosols of radiolabeled amphibole asbestos and found that the label was trated in "hot spots" adjacent to the visceral pleura at 104 and 139 da exposure. They suggested that these concentrations were due to translo fibers from the central regions of the lung toward the peripheral (sul regions. This process is often called "pleural drift."

The goals of the work presented here are to investigate whether plet occurs with chrysotile asbestos and to study the changes in fiber dim during the translocation process. In addition, this study seeks to desc clearance of chrysotile fibers from the rat lung. There are two reasons First, macrophage-mediated clearance of particles from pulmonary to bronchial region competes against transepithelial movement of particle interstitium (Ferin and Feldstein, 1978; Greenspan *et al.*, 1988). Thus an standing of clearance is a prerequisite for the investigation of fiber transl which may occur via the interstitium. Second, recent experimental w shown that longer (>5 μm) asbestos fiber preparations are more potent i of fibrosis than are shorter fibers (Adamson and Bowden, 1987a, 1987b; I *al.*, 1986; Davis and Jones, 1988). Differential clearance of these fiber p tions may explain some of their differential pathogenicity. Our findings r here show that both long and short chrysotile fibers are deposited by inhal peripheral and central regions of the rat lung. Subsequently, short fib cleared preferentially, and longer fibers remain in both regions of the lun

MATERIALS AND METHODS

Experimental design. Inhalation exposure methods have been describe ously (Warheit *et al.*, 1984a,b). Briefly, 23 adult male rats (Sprague–D specific pathogen free) of age 8–10 weeks were exposed for 3 hr to an aer 10 mg (respirable)/m^3 chrysotile asbestos. This is approximately 5000 fib μm in length/cm^3. Subgroups of four or five animals were sacrificed imme after exposure (0 days) and at 1, 8, 15, and 29 days postexposure. Four une animals were sacrificed 26 days after the exposure to serve as controls. A were sacrificed with an intraperitoneal injection of sodium pentobarbit

chest was opened and the pulmonary vasculature perfused with phosphate-buffered saline via the right ventricle. Lungs were fixed *in situ* by intratracheal instillation of 1% paraformaldehyde/1% glutaraldehyde in sodium cacodylate buffer, pH 7.2, at a pressure of 15 cm of water. Lungs were stored in fixative until dissection.

Lung dissection. The left lung was separated into peripheral and central regions under a dissecting microscope. The hilar portion of the left bronchus was discarded. The apical (~1 cm caudal to apex) and diaphragmatic (~2 mm cranial to diaphragmatic pleura) regions were resected as peripheral tissue. The remaining part of the left lung was cut transversely into ~2-mm-thick slices. Each slice was pinned to a dissecting board and the visceral pleura and a 1- to 2-mm-thick band of subpleural tissue was cut from the slice. The core of each slice comprised the central tissue. Peripheral and central tissue were separately minced into ~2-mm cubes with scissors. Excess fixative was removed by blotting, and tissue was placed into polypropylene centrifuge tubes. The wet weight of peripheral and central tissue was recorded for each animal. Control lungs were dissected in this manner as well.

For studies of deposition and translocation, fiber number and mass were divided by a normalization factor. This factor was calculated for a peripheral sample as $P/(P + C)$, where P and C are the wet weights of peripheral and central tissue, respectively. Peripheral tissue typically comprised 40% of the wet weight of the left lung; therefore the normalization factor was typically 0.4 for peripheral and [illegible] for central tissue.

Tissue digestion. Lung tissue was digested by a modification of the method of Williams *et al.* (1982). All reagents were filtered through 0.2-μm pore size membrane filters prior to use. Twenty milliliters of 12% sodium hypochlorite (NaOCl, Worth Chemical, Charlotte, NC) was added to each tube containing tissue. The tube was vortexed periodically and digestion allowed to progress for 30–45 min. The digest from each peripheral or central sample was divided equally and filtered onto two 25-mm-diameter, 0.2-μm pore size capillary pore filters (Nuclepore Corp., Pleasanton, CA). Lipids and other undigested debris were extracted by filtering a sequence of reagents: deionized water, isopropanol, 8% oxalic acid, 12% NaOCl, and a final rinse with deionized water. Filters were allowed to dry overnight in a desiccator.

The effect of the digestion procedure on fiber size distributions is described in Table 1. Portions of a suspension (in isopropanol) of 100 μg chrysotile asbestos/ml

TABLE 1
EFFECT OF DIGESTION PROCEDURE ON FIBER NUMBER, MASS, AND SIZE

	Standard suspension	Spiked digest
Fiber number	8.82×10^7	1.00×10^8
Fiber mass (μg)	7.07[a]	5.76[a]
Average fiber length (μm)	2.47	2.33
Average fiber diameter (μm)	0.118	0.108

[a] Recovery of standard suspension from tissue digest is 81% based on mass (5.76 μg/7.07 μg).

were either filtered directly or added to 1 g of lung tissue from an un animal. The tissue was digested as described above, and the fibers were e as described below. Recovery of chrysotile from the tissue was 81% b fiber mass. The digestion process caused a slight (~10%) increase in fiber and slight decreases in both average fiber length and average fiber diam

Microscopy. One wedge was cut from one of the two filters for each san mounted on a carbon disk with carbon paint. The sample was sputter coa gold for 2 min, then examined with a JEOL JSM-35 scanning electron micr 20-kV accelerating voltage, 15-mm working distance, 0° tilt, 5 sec/frame sc and magnification 4000–32,000× on the cathode ray tube (CRT, see belo

Fiber number and dimensions. The fiber number was determined by c the number of fibers present in fields (defined on the CRT by a rectangular randomly selected by traversing of the filter surface. Fibers were defined particle having aspect ratio ≥3:1 and having the morphology of a chrysotil In practice, almost all fibers encountered had aspect ratio ≥5:1. The N Institute of Occupational Safety and Health "B rules" were used for co whereby the number of fiber ends protruding into a defined field is count the result is divided by two to give the fiber number (Schneider, 1979). Succ fields were selected until at least 40 ends were counted in each lengt stratum (see below). The number of fields needed to reach this criteric recorded and used as the basis for the calculation according to the formu

$$\text{Fiber number} = \frac{(\text{fiber ends}) \times (\text{filter area})}{2 \times (\text{No. fields}) \times (\text{field area}) \times (\text{aliquot})}$$

"Aliquot" is the fraction of the sample on a given filter, here having the val (based on two filters per sample).

Fiber dimensions were measured by classification of each fiber encou into one of 48 length–diameter cells (Table 2). Each fiber was classified by at a given magnification using a transparent reticle with calibrated lines. L was based on the measurement of the fiber along its curve. The lowest length boundary (0.5 μm) was chosen on the basis of our confidence of fiber iden tion at 32,000× (32K×). Fibers shorter than 0.5 μm are present. Diameters classified at a screen magnification of 32K× using a reticle with calibrated c Generally, diameter was classified near the middle of a fiber, since the er chrysotile fibers tend to be splayed. Reticles were calibrated against a grid o lines/mm (Ernest Fullam, Latham, NY).

Stratified counting procedure. Starting at low magnification (100×), a st point was chosen near one edge of the filter. The magnification was then cha to 32K× and fiber ends of length (L) $0.5 \leq L < 1$ μm were counted and diameters classified. The number of ends in each diameter class was tabulat an eight-channel laboratory counter. A separate counter was used to tabulat number of fields. A new field was then chosen by moving the stage an arbi distance along the horizontal axis. Fields more than 30% obscured by debris not counted (less than 10% of all fields). New fields were chosen until the c criterion (40 ends) was reached or the edge of the filter was encountered. I

TABLE 2
LENGTH AND DIAMETER CLASSIFICATION

Magnification used for length classification:	32,000×	16,000×	16,000×	8,000×	8,000×	4,000×
Diameter (d)[a] class (μm)	Length (L) class (μm)[b]					
	$0.5 \leq L < 1$	$1 \leq L < 2$	$2 \leq L < 4$	$4 \leq L < 8$	$8 \leq L < 16$	$L \geq 16$
$d < 0.07$	0.75/0.06[c]	1.5/0.06	3/0.06	6/0.06	12/0.06	24/0.06
$0.07 \leq d < 0.10$	0.75/0.085	1.5/0.085	3/0.085	6/0.085	12/0.085	24/0.085
$0.10 \leq d < 0.14$	0.75/0.12	1.5/0.12	3/0.12	6/0.12	12/0.12	24/0.12
$0.14 \leq d < 0.20$	0.75/0.17	1.5/0.17	3/0.17	6/0.17	12/0.17	24/0.17
$0.20 \leq d < 0.28$	0.75/0.24	1.5/0.24	3/0.24	6/0.24	12/0.24	24/0.24
$0.28 \leq d < 0.40$	0.75/0.34	1.5/0.34	3/0.34	6/0.34	12/0.34	24/0.34
$0.40 \leq d < 0.57$	0.75/0.49	1.5/0.49	3/0.49	6/0.49	12/0.49	24/0.49
$d \geq 0.57$	0.75/0.69	1.5/0.69	3/0.69	6/0.69	12/0.69	24/0.69

[a] Diameter classes are based on a geometric progression: each class boundary is $\sqrt{2}\times$ the value of the next lowest boundary (0.07, 0.1, 0.14, . . .).

[b] Length classes are based on a geometric progression: each class boundary is twice the value of the next lowest boundary (0.5, 1, 2, . . .).

[c] The values in each cell are the length/diameter values used for calculations of average length, average diameter, and average mass.

latter case, the stage was repositioned along the vertical axis and the horizontal traversing continued in the opposite direction.

For other length classes fibers were identified and classified by length at the appropriate magnification (see Table 2) and then diameters were classified at 32K×. A separate eight-channel tabulator was used for each length class. Counting was continued for each length class until the criterion of 40 ends was reached. In this manner the statistical uncertainty due to sampling error was uniform across all length classes.

Calculations. A microcomputer-based spreadsheet program was used to perform all calculations. Fiber mass was based on the fiber number in each length–diameter cell assuming a cylindrical morphology:

$$\text{Mass} = \sum_{i,j} \pi N_{ij} L_i d_j^2 \rho / 4. \tag{2}$$

Here N_{ij} is the fiber number (calculated from formula (1) above) in the cell of length class i, diameter class j. L_i is the arithmetic midpoint of the ith length class, and d_j is the arithmetic midpoint of the jth diameter class (Table 2). The bulk density of chrysotile (ρ) is 2.55 gm/cm^3. The average fiber length and diameter were calculated according to the formulas below, where N_{total} is the total number of fibers in the sample:

$$\text{average length} = \sum_i \left(\sum_j N_{ij} \right) L_i / N_{\text{total}} \tag{3}$$

$$\text{average diameter} = \sum_i \left(\sum_i N_{ij} \right) d_i / N_{\text{total}}.$$

The formulas are approximations, since all fibers in a given size c assumed to have the same dimensions. However these formulas do re actual joint length–diameter distribution of the fibers.

We have tested the validity of the counting procedure by preparing a su (in isopropanol) of chrysotile fibers of known mass concentration and th ing a small aliquot for microscopic measurements. The mass calculated b scopic measurements, using formula (2), was 7.1 μg, while the mass kno gravimetric measurements was 12.2 μg.

Statistical analysis. The Systat microcomputer package was used for a tical analysis (Wilkinson, 1986). The clearance data (fiber number and ma log-transformed before analysis to equalize the variance at different time

RESULTS

Fiber Deposition in Peripheral and Central Regions

Both total (0 days postexposure) and pulmonary (1 day postexposure) tion were uniform between peripheral and central regions; i.e., normaliz number and mass were similar in each region (Table 3). Likewise, avera

TABLE 3
DEPOSITION IN PERIPHERAL AND CENTRAL REGIONS

	Total deposition (0 day postexposure) $n = 5$		Pulmonary depos (1 day postexpos $n = 4$	
	Peripheral (*P*)	Central (*C*)	Peripheral (*P*)	C
	Means across animals			
Fiber number[a] (normalized)	1.31×10^8	1.10×10^8	9.10×10^7	8.
Fiber mass (μg)[a] (normalized)	8.60	8.22	8.56	
Average fiber[b] length (μm)	1.47	1.57	1.65	
Average fiber[b] diameter (μm)	0.123	0.126	0.133	
	Summary statistics for each animal			
P:*C* ratio (mean[b] ± sem) fiber number	1.32 ± 0.32		1.05 ± 0.14	
P:*C* ratio (mean[b] ± sem) fiber mass	1.25 ± 0.38		1.00 ± 0.23	
Δ*C*-*P* (mean[b] ± sem) average length	0.100 ± 0.107		−0.053 ± 0.116	
Δ*C*-*P* (mean[b] ± sem) average diameter	0.003 ± 0.008		0.003 ± 0.006	

[a] Geometric mean across animals.
[b] Arithmetic mean across animals.

length and diameter were similar in the two regions (Table 3). In order to compare the deposition between the regions in a statistically valid manner, we formed summary statistics for each animal, i.e., ratios of peripheral/central for fiber number and mass, and central–peripheral differences for average fiber length and diameter (Table 3). None of these parameters was statistically different from 1.0 (number and mass ratios) or 0.0 (dimensional differences).

Translocation

Our working model for the translocation process is shown in Fig. 1. According to this model, if translocation occurs from central to peripheral regions, there will be an increase in the ratio of peripheral to central fibers over time. We therefore calculated the ratio of peripheral fiber mass to central fiber mass (both normalized to tissue wet weight as described under Materials and Methods) for each animal from 1 to 29 days postexposure (Fig. 2). There was no significant trend in the ratio over time. We also analyzed the trend of fiber mass and number ratio for each

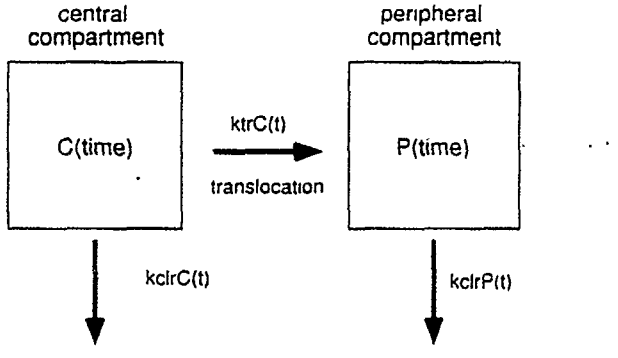

FIG. 1. Translocation model. $P(t)$ and $C(t)$ represent fiber burden in the peripheral and central regions as a function of time postexposure (t). The arrows represent fluxes. The flux out of a compartment is assumed to be proportional to the burden in that compartment. The flux from the central to the peripheral region is therefore $k_{tr}C(t)$, where k_{tr} is a constant. Clearance to the tracheobronchial region is assumed to follow the same first-order rate for each compartment, i.e., $k_{clr}P(t)$ and $k_{clr}C(t)$. Mass balance gives the following solutions for $P(t)$ and $C(t)$, where P_0 and C_0 are the initial burdens:

$$C(t) = C_0 e^{-(k_{clr}+k_{tr})t}$$
$$P(t) = [P_0 + C_0(1 - e^{-k_{tr}t})]e^{-k_{clr}t}.$$

This model predicts that the ratio $P(t)/C(t)$ will increase with time postexposure. Other models can give similar trends of lung burden in the two regions. In particular, a model can be formulated with no translocation but with slower clearance (rate k_p) from the peripheral region than from the central (rate k_c):

$$C(t) = C_0 e^{-k_c t}$$
$$P(t) = P_0 e^{-k_p t},$$

where $k_p < k_c$. This model also predicts that the ratio $P(t)/C(t)$ will increase with time postexposure. Generally, biologic data will not allow differentiation between the two models.

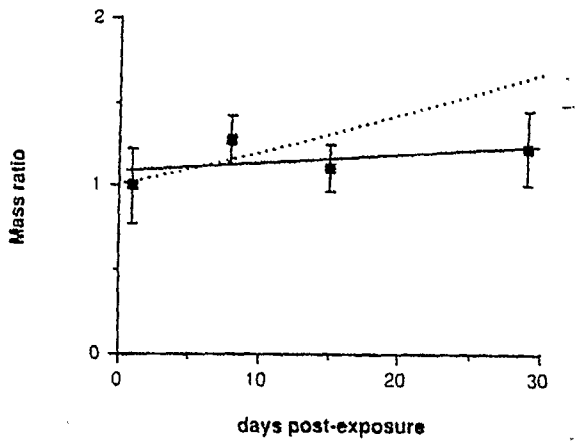

FIG. 2. Translocation: Plot of the ratio of normalized peripheral fiber mass to normalized fiber mass over time. The points are arithmetic means of the ratio, with standard errors indic the bars. The solid line is a linear regression of P/C ratio versus time. The slope of the lin significantly different from zero (p = 0.59). The dashed curve is the trend expected for a trans rate 20% of the overall clearance rate. This corresponds roughly to the upper 95% confidence the slope of the linear regression.

length class, from 0.5–1 μm to ≥16 μm. Again, there were no statistically icant trends (data not shown).

We performed a sensitivity analysis by applying the linear regression plot Fig. 2 to the translocation model. The 95% confidence limit of the slope linear regression corresponds roughly to a translocation rate of 20% of the o clearance rate (half-life ~ 13 days) in terms of fiber mass. Thus this exper put an upper bound on the translocation rate of ~0.01 day^{-1}, correspondin process with a half-life of 73 days (half-life = ln 2/translocation rate).

The 0-day time point was excluded from calculations *a priori* because the burden then includes fibers in the tracheobronchial region. We were only ested in translocation and clearance in the slow-clearing or pulmonary re Inspection of the data, however, showed that none of our conclusions wou altered substantially by inclusion of the 0-day time point.

Clearance

For analysis of clearance, we summed peripheral and central fiber numb length–diameter cell for each animal. Therefore clearance rates are based o fiber burden for the entire left lobe. Again, we exclude the time point at 0 postexposure, but its inclusion would not alter any conclusions substantiall

In previous work, we plotted length and diameter distributions of chrys fibers retained in the lung at different times postexposure and showed tha tained fibers are progressively narrower and longer as time increases (Roggli Brody, 1984). Log-probability plots of length and diameter confirm this in present study (data not shown). The changes in size distributions are also ap ent in micrographs of digests (Fig. 3). A plot of total fiber mass versus

postexposure can be fit with a two-compartment clearance model (Fig. 4), in agreement with previous work from this laboratory (Roggli and Brody, 1984).

The length-stratified counting scheme permits a more informative analysis. Figure 5 shows plots of fiber number versus time postexposure for each length class separately. These plots show that the number of fibers of all classes <8 μm in length decreased over time. In contrast, fiber number in the 8- to 16-μm class did not change significantly up to 29 days postexposure, and the number of fibers greater than 16 μm in length *increased* significantly. It is likely that two phenomena explain these results: (1) The clearance rate is inversely related to fiber length, (2) fibers undergo longitudinal splitting over time.

Figure 6 shows that average fiber diameter decreases over time within each length class, consistent with longitudinal splitting of all length classes of fibers. In order to correct for longitudinal splitting, we calculated fiber mass within each length class and plotted clearance curves (Fig. 7). (If fibers split only longitudinally, the mass within each length class will be conserved. This is an approximation, since transverse splitting of fibers probably occurs as well—see Discussion.) For each length class we calculated a clearance rate and half-life based on a one-compartment model. The clearance half-lives increased with increasing fiber length: ~10 days for fibers 0.5–4 μm, increasing to 114 days for fibers ≥16 μm. Statistically, the clearance rate for fibers greater than 16 μm was not significantly different from zero (half-life infinity). These results are summarized in Fig. 8.

DISCUSSION

Deposition in Peripheral and Central Regions

The lack of differential deposition between peripheral and central regions of the rat lung was surprising. On the basis of two previous experimental findings, we expected that there would be greater deposition in the central than in the peripheral region. First, deposition of chrysotile asbestos occurs preferentially at first alveolar duct bifurcations (Brody *et al.*, 1981), and we expected there to be a higher density of these bifurcations in central compared to peripheral tissues. Second, asbestos fiber deposition in a given region of the pulmonary parenchyma is inversely related to the pathlength (as measured from the carina) of the airway supplying that region (Pinkerton *et al.*, 1986), and we expected the average airway pathlength to be greater in the peripheral than in the central region.

In view of the present experimental findings, we examined histologic sections from rat lungs and found that first alveolar duct bifurcations can occur within 0.5 mm of the visceral pleura. Therefore, our dissection scheme is too crude to exclude many first duct bifurcations from "peripheral" tissue. A quantitative assessment of the density of first alveolar duct bifurcations in peripheral versus central regions would require morphometric analysis. Similar considerations may apply to airway pathlength. The dissection scheme used here does not reveal differences in pathlength between peripheral and central regions.

Total (0 day postexposure) and pulmonary (1 day postexposure) deposition of chrysotile were similar (Table 3), indicating that little, if any, of the chrysotile burden measured represents fibers deposited in the ciliated airways.

Translocation

This study provides no evidence for the translocation of chrysotile fibers toward the peripheral region or for preferential clearance of fibers from one region. Sensitivity analysis (see Results) suggests that, if translocation occurs, the rate can be no greater than 20% of the overall clearance rate. This finding does not agree with that of Morgan *et al.* (1977), who observed subpleural concentrations of asbestos in rats exposed by inhalation. However, there are significant differences between that study and the present one. Morgan *et al.* (1977) employed amphiboles (crocidolite and a synthetic fluoramphibole), and the observations of subpleural hot spots were made at 104 and 139 days postexposure, three to four times the follow-up of our study. Translocation may be a slow process, and our study may not have had sufficient follow-up time to detect it. Furthermore, some experimental work suggests that inhaled crocidolite may produce a more severe subpleural reaction, including retention of fibers in localized lesions, than does chrysotile (Oghiso *et al.*, 1984).

In addition, our dissection and digestion technique cannot differentiate between translocation from central to peripheral regions and slower clearance from the peripheral region relative to the central. In both cases, the ratio of peripheral to central fiber burden should increase over time. Likewise, autoradiographic techniques such as those used by Morgan *et al.* (1977) suffer from the same limitations. An area of intense autoradiographic signal at one time point cannot be compared to the signal at another time point if the development times of the autoradiographs are different, as was the case in that study. Only a relative comparison of signal within a single autoradiograph is appropriate. Therefore the hot spots observed in that study may represent areas of slower clearance of deposited fibers and not concentrations of fibers translocated from other regions. These hot spots may correspond to asbestos-induced inflammatory lesions observed by others (Oghiso *et al.*, 1984).

Another limitation of the present work is the possibility that translocation of particles to the pleural regions occurs only at lung burdens much higher than those achieved here. Translocation of particles to the hilar lymph nodes of the rat increases when clearance mechanisms are overloaded at lung burdens of approximately 1 mg (Ferin and Feldstein, 1978; Strom *et al.*, 1989). Particle translocation to the pleura may occur through the lymphatics (Hillerdal, 1980), so these findings may be relevant to the present work. Our study used a very modest exposure to chrysotile (10 mg/m^3 for 3 hr), which gives an initial lung burden of ~10 μg in the left lung (Table 2) or ~30 μg for all lobes of the rat lung. This is well below the burden of asbestos (~1.5 mg) associated with clearance overload in the rat (Bol-

FIG. 3. Micrographs of lung digests. (A) Scanning electron micrograph (SEM) of lung digest from an animal sacrificed 1 day postexposure. Many short (<5 μm) fibers are present. Average fiber diameter is ~0.13 μm. Note the long, wide (length >20 μm, diameter ~0.5 μm) fiber at the top of the micrograph. (B) SEM of lung digest from an animal sacrificed 29 days postexposure. Fewer short (<5 μm) fibers are present (arrows) than at 1 day. Average fiber diameter is ~0.09 μm. Note the long, narrow (length >20 μm, diameter ~0.1 μm) fiber at the top of the micrograph.

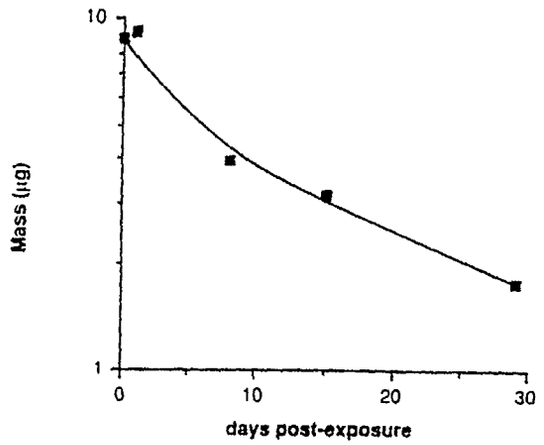

FIG. 4. Clearance in terms of mass. The points represent geometric means across animal: left lobe burden. Mass was calculated according to Eq. (2) in the text. The curve is a fit c compartment model to the data:

$$M(t) = M_0[\alpha e^{-k_1 t} + (1 - \alpha)e^{-k_2 t}].$$

Here $M(t)$ is fiber mass as a function of time, M_0 is the initial burden, α is the fraction of mass d in compartment 1, k_1 is the clearance constant for compartment 1, and k_2 is the clearance con compartment 2. The best-fit model has values $\alpha = 0.45$, $k_1 = 0.24$ (half life 3 days), $k_2 = 0.0$ life 20 days). The parameters were derived by least-squares fit to the log-transformed mass b The value of M_0 was forced to the geometric mean of the initial value (8.7 μg). The geometr of fiber mass in the four control animals was 0.11 μg.

ton *et al.*, 1983). Note, however, that Morgan *et al.* (1977) observed "p drift" after modest inhalation exposures (a maximum of 50 mg/m^3 for 30 giving initial lung burdens on the order of 10–20 μg, comparable to the bu obtained in our study.

Clearance

The clearance rate of chrysotile fibers is inversely related to fiber length. clearance rate of fibers greater than 16 μm in length is very low and not si cantly different from zero in this study. These observations would have been difficult without the use of the length-stratified counting technique. Asb fibers have a lognormal length distribution. Proper description of such a dist tion requires that either a great number of fibers be measured or that a strat sampling scheme be used. For example, in typical lung digests, fibers of le greater than 16 μm constitute 0.3% of the total number present. Our strat counting scheme ensures acceptable statistical accuracy by obtaining a count least 20 fibers in this class. Using this scheme, characterization of the le distribution between 0.5 and 16 μm requires counting between 120 and 240 fi (six length classes × 20–40 fiber ends/class). In contrast, achieving this leve accuracy by measuring every fiber encountered in a random search would req

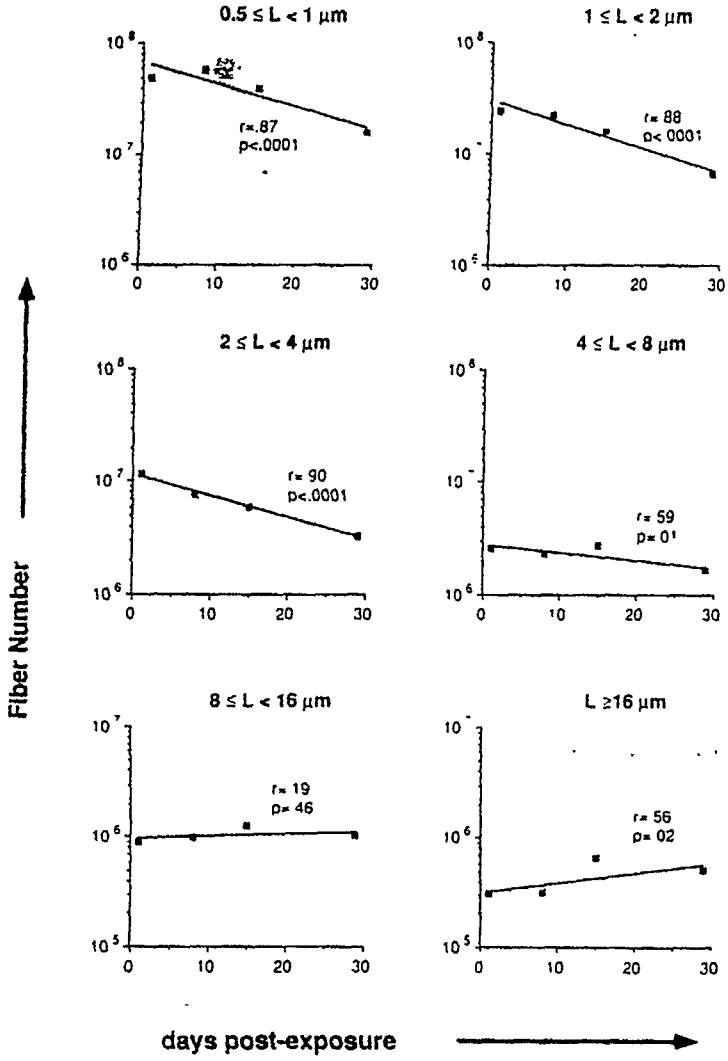

FIG. 5. Fiber number by length class. The points plotted are geometric means of fiber number within a length class. The lines are linear regressions of log-transformed fiber number for each animal. These can be interpreted as fits of a one-compartment clearance model for each length class: $N_i(t) = N_{i0}e^{-k_i t}$, where $N_i(t)$ is the fiber number in length class i as a function of time (t). N_{i0} is the initial pulmonary deposition in length class i, and k_i is a clearance constant. Statistical significance (p) and correlation (r) are shown with each graph. Fiber number is decreasing significantly over time for each length class under 8 μm. For the class 8–16 μm, fiber number is not changing significantly over time. For the class ≥16 μm, fiber number is *increasing* significantly over time. The geometric mean of total fiber number in control animals was 7×10^5. For each length class the control value was well below that of the exposed animals. For example the mean control value for fibers ≥16 μm was 3×10^3, less than 1/100 the value in exposed animals.

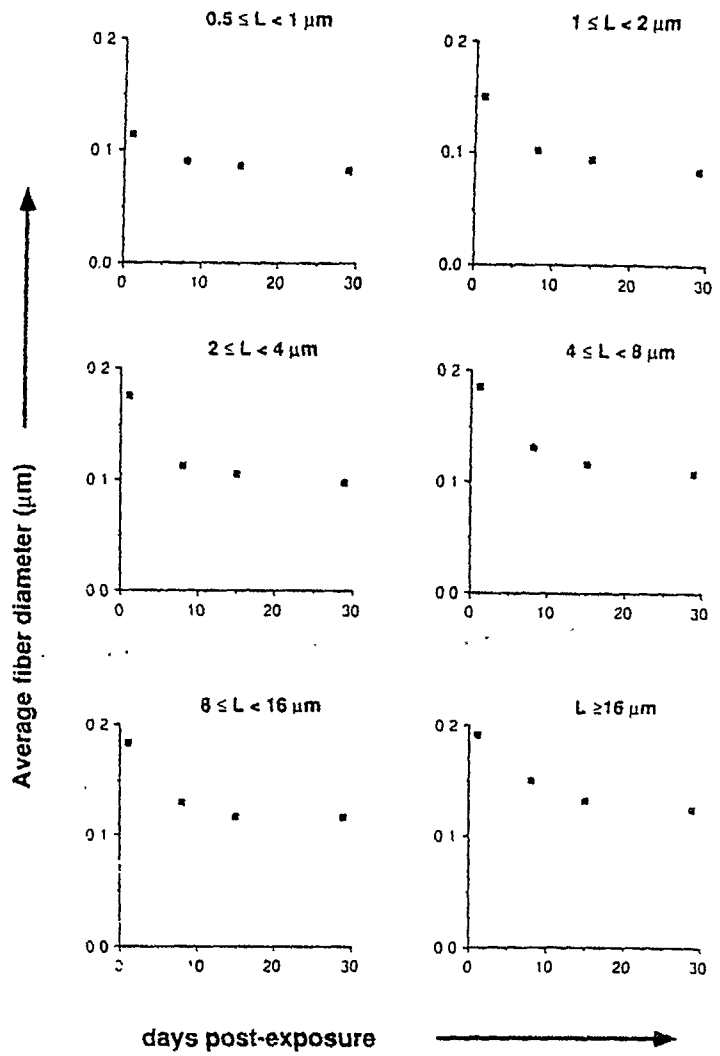

FIG. 6. Average fiber diameter by length class. Average fiber diameter was calculated acro mals for each length class according to a modification of Eq. (4). The plotted points are anti means across animals.

measurement of approximately 7000 fibers. (The total fibers counted to give the ≥16 µm class is ≈20/0.003 = 6700.)

In addition, the length-dependent clearance observed here is not a resu overload of the pulmonary clearance system. The lung burdens achieved in study are much lower than those associated with clearance overload (see dis sion above under Translocation).

Interpretation of the clearance curves is complicated by the tendenc

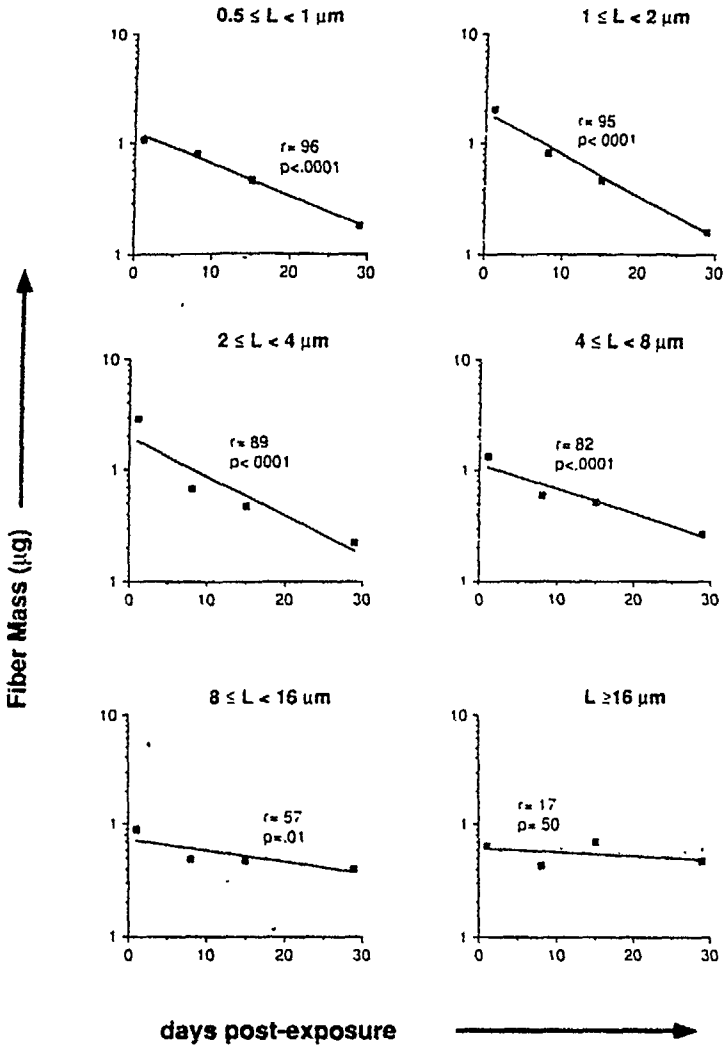

FIG. 7. Fiber mass by length class. The points plotted are geometric means of fiber mass within a length class. The lines are linear regressions of log-transformed fiber mass for each animal. These can be interpreted as fits of a one-compartment clearance model for each length class: $M_i(t) = M_{i0}e^{-k_i t}$, where $M_i(t)$ is the fiber mass in length class i as a function of time (t). M_{i0} is the initial pulmonary deposition in length class i, and k_i is a clearance constant. Statistical significance (p) and correlation (r) are shown with each graph. Fiber mass is decreasing significantly over time for each length class under 16 µm.

chrysotile fibers to split. The length and diameter of a fiber may change during its residence in the lung, independent of any mechanical clearance to the tracheobronchial region. Thus, splitting may alter the apparent clearance rate of fibers within a certain length class. We corrected for longitudinal splitting (which will

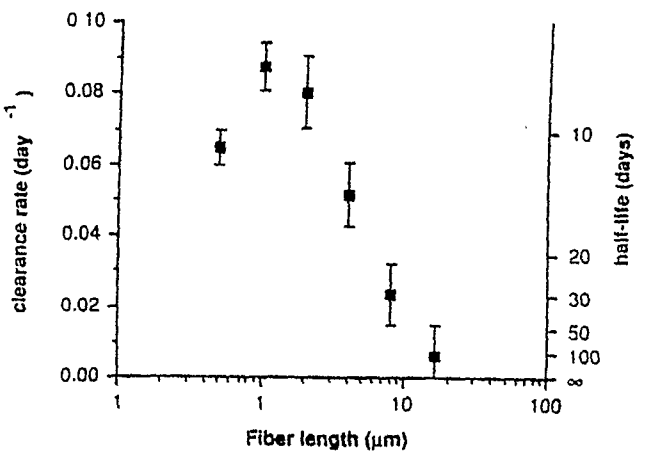

FIG. 8. Summary of clearance rate by fiber length. The points plotted are values of th compartment clearance model based on the mass curves of Fig. 7. The value of fiber length pl the lower end of the length class. The error bar represents the standard error of the estimate ba the linear regression. The scale on the right shows the half life ($t_{1/2}$) coresponding to the cle constant (k) on the left-hand scale ($t_{1/2} = \ln 2/k$).

not change the length of a fiber) by calculating clearance rates based on fiber within each length class. This correction was successful for the fibers greater 16 μm in length. Their clearance rate (based on fiber mass) is near zero, sugge that a great deal of transverse splitting did not occur. On the other hand clearance rate of the 0.5- to 1-μm length class was somewhat lower than exp based on the trend of clearance rate versus fiber length (Fig. 8). This anom probably due to splitting of larger fibers into fragments of length 0.5–1 μm.

Other experimental work concurs with our finding of length-dependent c ance. Many workers have noted that the average length of fibers retained i lung increases over time in experimental animals (Kimizuka *et al.*, 1987; R and Brody, 1984; Roggli *et al.*, 1987). Such changes in size distribution are sistent with length-dependent clearance. Clearance of amosite from the lun hamsters shows a dependence on fiber length almost identical to that found i present study (Coin *et al.*, 1990). Morgan *et al.* (1982) found that preparatio glass fibers between 5 and 10 μm in length were cleared from the rat lung half-lives of 60–90 days, while fibers of 30 μm length were not cleared. Tim (1981) compared size distributions of anthophyllite fibers in aerosol samples that in the lungs of exposed humans and concluded that fibers greater than 1 in length were not cleared.

Pulmonary clearance of isometric particles also depends on particle size experimental animals, isometric particles greater than 7–9 μm in diameter cleared slowly, if at all, from the pulmonary region (Snipes and Clem, 1 Snipes *et al.*, 1984). This is likely due to the inability of pulmonary alve macrophages (PAM) to phagocytize and/or transport these particles. Mor (1988) suggests PAM may become immobilized after engulfing more than a cri

lume (~60–600 μm^3/PAM) of isometric particles. This corresponds to a single particle of between 5 and 11 μm diameter, similar to the clearance limit observed *in vivo*.

On the basis of the present work, we suggest that immobilization of PAM (or failure of phagocytosis) may occur upon attempted phagocytosis of a particle greater than a certain *dimension*. In our experiment, chrysotile fibers greater than 16 μm in length are not cleared at a significant rate. These fibers have an average diameter (at deposition) of ~0.2 μm, giving a typical volume of only 0.5 μm^3, well below the volumetric limit for clearance proposed for isometric particles (Morrow, 1988). Our proposed dimensional limit for the clearance of fibers correlates with the size of PAM, which are 10–20 μm in diameter (Warheit *et al.*, 1984b; Fels and Cohn, 1986). Possibly PAM cannot engulf fibers which are longer than their own cell diameter, and/or PAM become immobile after phagocytosis of such fibers.

Slower clearance of longer fibers may explain the increased pathogenicity of long fiber preparations compared to short (Adamson and Bowden, 1987a, 1987b; Davis *et al.*, 1986; Davis and Jones, 1988). Prolonged retention of asbestos fibers in the lung leads to development of asbestosis in an animal model (Begin and Sebastien, 1989). Thus, other factors being equal, a preparation of long fibers will be retained in the lung for a greater length of time and should cause more fibrosis than a preparation of short fibers.

The length dependence of clearance needs to be considered in human studies correlating fiber burden with pathology. For example, Churg and co-workers have found that average fiber length of asbestos burden is negatively correlated with grade of fibrosis (Churg *et al.*, 1989, 1990). They suggest several explanations for this observation, including that short fibers are "important generators of fibro-" or alternatively, that "preferential retention of short fibers would have to occur" in areas of fibrosis. The results of our work and that of others suggest the latter explanation is plausible. We showed that fibers greater than 16 μm in length were cleared very slowly, if at all. This length dependence of clearance occurred in the absence of extensive pulmonary fibrosis and inflammation, which may inhibit clearance (Tryka *et al.*, 1985; Slauson *et al.*, 1989). The magnitude of asbestos exposure used here produces lesions only at the alveolar duct bifurcations and does not cause generalized pulmonary inflammation (Brody *et al.*, 1981; Warheit *et al.*, 1984a; Chang *et al.*, 1988). Furthermore, in other animal models of asbestosis, generalized pulmonary fibrosis and suppression of clearance (overload) occur at much higher lung burdens (~1.5 mg) (Bolton *et al.*, 1983) than those achieved here (~30 μg). Therefore, if any suppression of clearance occurs due to fibrosis or inflammation it will affect primarily the clearance of shorter fibers, since longer ones are not cleared, as discussed above. This means that suppression of fiber clearance for any reason will cause a *decrease* in the average length of retained fibers.

Experimental results cannot rule out the possibility that, in humans, short fibers are important in causing fibrosis (Churg *et al.*, 1989, 1990). It is quite possible, as suggested by others (Churg *et al.*, 1990; Goodglick and Kane, 1990), that short fibers contribute to fibrosis and other diseases once inflammation and/or impair-

ment of clearance occurs. This hypothesis could be tested experiment pulmonary fibrosis, but has not been addressed to date. For example, could be exposed to a short fiber preparation in combination with an agen produces inflammation and retards clearance of particles.

CONCLUSIONS

The results of the present study could have implications for the pathoge asbestos-related pleural disease. While we found no evidence of pleural d did find that substantial numbers of inhaled fibers are deposited within 1–2 the visceral pleura of the rat. Many are probably deposited within a few h micrometers of the visceral pleura. These include fibers greater than 16 length, which are cleared slowly, if at all. Indeed their number *increased* ov due to longitudinal splitting (Fig. 5). These fibers may be susceptible t translocation processes not detectable in this study. Thus subpleural fibe not move far or fast in order to reach the vicinity of the visceral pleura. Fi this region could cause inflammation in the subpleural parenchyma, thereb ing pleural disease. In concordance with this hypothesis, ongoing work laboratory indicates that, in mice exposed for 5 hr to 10 mg/m^3 of chr subpleural peripheral mesenchymal cells show enhanced uptake of tritiat midine within 24 hr of inhalation exposure (Coin *et al.*, 1991). Studies are way to determine if this proliferative response is due to the presence of fil the subpleural layer and/or the diffusion of growth factors released by e cells at first alveolar duct bifurcations (McGavran *et al.*, 1990; Bonner 1990).

ACKNOWLEDGMENTS

This work was supported by Department of Veterans Affairs Medical Research Funds. Haseman of the National Institute of Environmental Health Sciences reviewed the statistical a

REFERENCES

Adamson, I. Y. R., and Bowden, D. H. (1987a). Response of mouse lung to crocidolite asbe Minimal fibrotic reaction to short fibres. *J. Pathol.* 152, 99–107.

Adamson, I. Y. R., and Bowden, D. H. (1987b). Response of mouse lung to crocidolite asbe Pulmonary fibrosis after long fibres. *J. Pathol.* 152, 109–117.

Begin, R., and Sebastien, P. (1989). Excessive accumulation of asbestos fibre in the bronchoa space may be a marker of individual susceptibility to developing asbestosis: Experimen dence. *Br. J. Ind. Med.* 46, 853–855.

Bolton, R. E., Vincent, J. H., Jones, A. D., Addison, J., and Beckett, S. T. (1983). An ov hypothesis for pulmonary clearance of UICC amosite fibres inhaled by rats. *Br. J. Ind. M* 264–272.

Bonner, J. C., Badgett, A., Osornio-Vargas, A. R., Hoffman, M., and Brody, A. R. (1990). stimulated fibroblast proliferation is enhanced synergistically by receptor-recognized α_2- globulin. *J. Cell. Physiol.* 145, 1–8.

Brody, A. R., Hill, L. H., Adkins, B., and O'Connor, R. W. (1981). Chrysotile asbestos inhala rats: Deposition pattern and reaction of alveolar epithelium and pulmonary macrophage *Rev. Respir. Dis.* 123, 670–679.

Brody, A. R., and Roe, M. W. (1983) Deposition pattern of inorganic particles at the alveolar l the lungs of rats and mice. *Am. Rev. Respir. Dis.* 128, 724–729.

and extracellular matrix production after a brief exposure to asbestos. *Am. J. Pathol.* 131, 156–170.

Churg, A., and Wiggs, B. (1987). Accumulation of long asbestos fibers in the peripheral upper lobe in cases of malignant mesothelioma. *Am. J. Ind. Med.* 11, 563–569.

Churg, A., Wright, J., Depaoli, L., and Wiggs, B. (1989). Mineralogic correlates of fibrosis in chrysotile miners and millers. *Am. Rev. Respir. Dis.* 139, 891–896.

Churg, A., Wright, J., Wiggs, B., and Depaoli, L. (1990). Mineralogic parameters related to amosite asbestos-induced fibrosis in humans. *Am. Rev. Respir. Dis.* 142, 1331–1336.

Coin, P. G., Moore, L. B., Roggli, V. L., and Brody, A. R. (1991). Pleural incorporation of ^{3}H-TdR after inhalation of chrysotile asbestos in the mouse. *Am. Rev. Respir. Dis.* 143, A604.

Coin, P. G., Stevens, J. B., and McJilton, C. M. (1990). Role of fiber length in the pulmonary clearance of amosite asbestos. *Am. Rev. Respir. Dis.* 141, A521.

Davis, J. M. G., Addison, J., Bolton, R. E., Donaldson, K., Jones, A. D., and Smith, T. (1986). The pathogenicity of long versus short fibre samples of amosite asbestos administered to rats by inhalation and intraperitoneal injection. *Br. J. Exp. Pathol.* 67, 415–430.

Davis, J. M. G., and Jones, A. D. (1988). Comparisons of the pathogenicity of long and short fibres of chrysotile asbestos in rats. *Br. J. Exp. Pathol.* 69, 717–737.

Dodson, R. F., and Ford, J. O. (1985). Early response of the visceral pleura following asbestos exposure: An ultrastructural study. *J. Toxicol. Environ. Health* 15, 673–686.

Fels, A. O. S., and Cohn, Z. A. (1986). The alveolar macrophage. *J. Appl. Physiol.* 60, 353–369.

Ferin, J., and Feldstein, M. L. (1978). Pulmonary clearance and hilar lymph node content in rats after particle exposure. *Environ. Res.* 16, 342–352.

Goodglick, L. A., and Kane, A. B. (1990). Cytotoxicity of long and short crocidolite asbestos fibers *in vitro* and *in vivo*. *Cancer Res.* 50, 5153–5163.

Greenspan, B. J., Morrow, P. E., and Ferin, J. (1988). Effects of aerosol exposures to cadmium chloride on the clearance of titanium dioxide from the lungs of rats. *Exp. Lung Res.* 14, 491–499.

Hill, R. J., Edwards, R. E., and Carthew, P. (1990). Early changes in the pleural mesothelium following intrapleural inoculation of the mineral fibre erionite and the subsequent development of mesotheliomas. *J. Exp. Pathol.* 71, 105–118.

Hillerdal, G. (1980). The pathogenesis of pleural plaques and pulmonary asbestosis: Possibilities and impossibilities. *Eur. J. Resp. Dis.* 61, 129–138.

Jaurand, M-C., Fleury, J., Monchaux, G., Nebut, M., and Bignon, J. (1987). Pleural carcinogenic potency of mineral fibers (asbestos, attapulgite) and their cytotoxicity on cultured cells. *J. Nat. Cancer Inst.* 79, 797–804.

Kimizuka, G., Wang, N-S., and Hayashi, Y. (1987). Physical and microchemical alterations of chrysotile and amosite asbestos in the hamster lung. *J. Toxicol. Environ. Health* 21, 251–264.

Lapin, C. A., Craig, D. K., Valerio, M. G., McCandless, J. B., and Bogoroch, R. (1991). A subchronic inhalation toxicity study in rats exposed to silicon carbide whiskers. *Fund. Appl. Toxicol.* 16, 128–146.

Mavran, P. D., Moore, L. B., and Brody, A. R. (1990). Inhalation of chrysotile asbestos induces rapid cellular proliferation in small pulmonary vessels of mice and rats. *Am. J. Pathol.* 136, 695–705.

Morgan, A., Evans, J. C., and Holmes, A. (1977). Deposition and clearance of inhaled fibrous minerals in the rat. Studies using radioactive tracer techniques. *In* "Inhaled particles IV" (W. H. Walton, Ed.), pp. 259–272. Pergamon, Oxford.

Morgan, A., Holmes, A., and Davison, W. (1982). Clearance of sized glass fibres from the rat lung and their solubility *in vivo*. *Ann. Occup. Hyg.* 25, 317–331.

Morrow, P. E. (1988). Possible mechanisms to explain dust overloading of the lungs. *Fund. Appl. Toxicol.* 10, 369–384.

Oghiso, Y., Kagan, E., and Brody, A. R. (1984). Intrapulmonary distribution of inhaled chrysotile and crocidolite asbestos: Ultrastructural features. *Br. J. Exp. Pathol.* 65, 467–484.

Pinkerton, K. E., Brody, A. R., McLaurin, D. A., Adkins, B., O'Connor, R. W., Pratt, P. C., and Crapo, J. D. (1983). Characterization of three types of chrysotile asbestos after aerosolization. *Environ. Res.* 31, 32–53.

Pinkerton, K. E., Plopper, C. G., Mercer, R. R., Roggli, V. L., Patra, A. L., Brody, Crapo, J. D. (1986). Airway branching patterns influence asbestos fiber location and th tissue injury in the pulmonary parenchyma. *Lab. Invest.* 55, 688–695.

Roggli, V. L., and Brody, A. R. (1984). Changes in numbers and dimensions of chrysotil fibers in lungs of rats following short-term exposure. *Exp. Lung Res.* 7, 133–147.

Roggli, V. L., George, M. H., and Brody, A. R. (1987). Clearance and dimensional chan cidolite asbestos fibers isolated from lungs of rats following short-term exposure. *Env* 42, 94–105.

Schneider, T. (1979). The influence of counting rules on the number and on the size distr fibers. *Ann. Occup. Hyg.* 21, 341–350.

Sebastien, P., Janson, X., Gaudichet, A., Hirsch, A., and Bignon, J. (1980). Asbestos re human respiratory tissues: Comparative measurements in lung parenchyma and in pariet *In* "Biological Effects of Mineral Fibres" (J. C. Wagner, Ed.), pp. 237–246. W.H.O./ Lyon.

Slauson, D. O., Lay, J. C., Castleman, W. L., and Neilsen, N. R. (1989). Acute inflamma injury retards pulmonary particle clearance. *Inflammation* 13, 185–199.

Snipes, M. B., Chavez, G. T., and Muggenburg, B. A. (1984). Disposition of 3-, 7-, and 1 crospheres instilled into lungs of dogs. *Environ. Res.* 33, 333–342.

Snipes, M. B., and Clem, M. F. (1981). Retention of microspheres in the rat lung after intr instillation. *Environ. Res.* 24, 33–41.

Stanton, M. F., Layard, M., Tegeris, A., Miller, E., May, M., Morgan, E., and Smith, A Relation of particle dimension to carcinogenicity in amphibole asbestos and other fibrou als. *J. Nat. Cancer Inst.* 67, 965–975.

Strom, K. A., Johnson, J. T., and Chan, T. L. (1989). Retention and clearance of inhaled su carbon black particles. *J. Toxicol. Environ. Health* 26, 183–202.

Suzuki, Y., and Kohyama, N. (1991). Translocation of inhaled asbestos fibers from the lung tissues. *Am. J. Ind. Med.* 19, 701–704.

Timbrell V. (1982). Deposition and retention of fibres in the human lung. *Ann. Occup. H* 347–369.

Tryka, A. F., Sweeney, T. D., Brain, J. D., and Godleski, J. J. (1985). Short-term regional cl of an inhaled submicrometric aerosol in pulmonary fibrosis. *Am. Rev. Respir. Dis.* 132, 6

Viallat, J. R., Raybuad, F., Passarel, M., and Boutin, C. (1986). Pleural migration of chrysotil after intratracheal injection in rats. *Arch. Environ. Health* 41, 282–286.

Warheit, D. B., Chang, L. Y., Hill, L. H., Hook, G. E. R., Crapo, J. D., and Brody, A. R. (Pulmonary macrophage accumulation and asbestos-induced lesions at sites of fiber dep *Am. Rev. Respir. Dis.* 129, 301–310.

Warheit, D. B., Hill, L. H., and Brody, A. R. (1984b). Surface morphology and correlated pha capacity of pulmonary macrophages lavaged from the lungs of rats. *Exp. Lung Res.* 6, 71

Warheit, D. B., and Hartsky, M. A. (1990). Species comparisons of proximal alveolar dep patterns of inhaled particulates. *Exp. Lung Res.* 16, 83–99.

Wilkinson, L. (1986). "SYSTAT: The System for Statistics." SYSTAT, Inc. Evanston, IL.

Williams, M. G., Dodson, R. F., Corn, C., and Hurst, G. A. (1982). A procedure for the isola amosite asbestos and ferruginous bodies from lung tissue and sputum. *J. Toxicol. Environ.* 10, 627–638.